A Pareto Frontier-Based Multi-Objective Chaotic PSO with Sigmoid-based Acceleration Coefficients for Optimal DG Placement and Sizing

Rajesh Murari[1], *and* Srinivasa Rao Rayapudi[2], *Sr. Member, IEEE*

***Abstract*— The escalating demand for electric power necessitates an expansion of electric power networks, posing technical, economic, and environmental challenges. Renewable energy sources like solar photovoltaics and wind generators offer potential solutions by integrating into power grids. The optimal placement and sizing of distributed generation (DG) within distribution networks (DNs) profoundly affect various factors such as power loss, voltage stability, and voltage deviation. This article presents a multi-objective chaotic PSO with sigmoid-based (MO-CPSOS) acceleration coefficient algorithm with Pareto frontier approach for optimal DG placement and sizing for the first time. The MO-CPSOS algorithm is tested for the standard IEEE 33-bus, 69-bus, and 118-bus systems. Simulation results demonstrate the efficacy of the proposed approach with a single objective in terms of power loss reduction, optimal DG size, and convergence speed. Further, investigations suggest that MO-CPSOS algorithm with multi-objective achieves competitive results in power loss and voltage deviation minimization, and voltage stability enhancement compared to existing methods.**

***Index Terms*— Chaotic PSO, Distributed Generation, Multi-Objective Approach, Power Loss, Pareto Front.**

NOMENCLATURE

P_{jk}, Q_{jk}	Power flows between *bus-j* and *bus-k*
B_{jm}, G_{jm}	Components of line impedance matrix Z_{jm}
r_{jk}, x_{jk}	Resistance and reactance of *line-jk*
V_j, V_k	Voltage magnitudes at *bus-j* and *k*
P_j, Q_j	Real and reactive power injections at *bus-j*
P_{demand}, P_{dg}	Real power demand and generation by DG
max, min	Maximum and minimum, respectively
RPLI	Real Power Loss Index
SVDI	System Voltage Deviation Index
SVSI	System Voltage Sensitivity Index
TRPL	Total Real Power Loss
V_{rated}	Bus rated voltage (1.0 p.u.)
PSO	Particle Swarm Optimization
x_i, v_i	Position and velocity of i^{th} particle in PSO,
p_{best}, g_{best}	Particle best and global best in PSO
c_p, c_g	Cognitive and social coefficients
r_1, r_2	Random values between 0 and 1
ω	Inertia weight
τ, τ_{max}	Current and maximum Iteration number

I. INTRODUCTION

THE increasing demand for electric power and the imperative for widespread access necessitate a rapid expansion of electric power networks. This growth presents technical, economic, and environmental challenges. Renewable energy sources, such as solar photovoltaics and wind generators, offer the potential to reduce reliance on conventional energy sources when integrated into the power grid. India, with its substantial distributed generation (DG) potential can significantly impact its economy and decrease emissions [1]. The strategic placement and sizing of DGs profoundly impact power loss, voltage stability, voltage deviation, service reliability, power quality, cost, and environmental impact [2][3].

In the quest to address the optimal placement and sizing of DG within distribution networks (DNs), researchers have adopted a diverse array of optimization techniques, mathematical, analytical, heuristic, and meta-heuristic approaches. Mathematical approaches such as mixed-integer linear programming have been applied to determine the optimal DGs size. These methods necessitate the linearization of non-linearities inherent in power flow equations, introducing approximations that may affect the model's accuracy. Analytical approaches, such as sensitivity methods have also been proposed for optimal DG placement. These methods primarily focus on identifying optimal DG locations, while sizing is determined through loss minimization strategies. However, it's worth noting that while these techniques utilize gradients for optimal DG locations, they may not guarantee a global optimal solution.

As the demand for efficient solutions intensifies, meta-heuristic approaches have emerged as favored methodologies. A plethora of these algorithms including differential evolution (DE) [4], PSO [5], ant lion optimization (ALO) algorithm [6], coot bird optimization method (CBOM) [7], equilibrium optimizer (EO) [8] have been explored. These techniques have found extensive application in DG placement and sizing with loss minimization as single (primary) objective. However, many of these studies have predominantly focused on relatively modest sizes, such as the 33-bus and 69-bus systems.

To address the limitations of single-objective optimization, some researchers have proposed multi-objective approach

[1] Department of Electrical & Electronics Engineering, Aditya University, Surampalem & Scholar at JNTUK, Kakinada, AP, India.

[2] Department of Electrical & Electronics Engineering, Jawaharlal Nehru Technological University Kakinada (JNTUK), Kakinada, AP, India 533003 .

using backtracking search optimization algorithm (BSOA) [9], flower pollination algorithm (FPA) [10], elephant heard optimization (EHO) [11], whale optimization algorithm (WOA) [12]. These approaches aim to simultaneously optimize multiple conflicting objectives often employing weighted sum methods to obtain optimal solutions. However, these algorithms also face challenges related to premature convergence and slow convergence rate, particularly when applied to larger networks.

In contrast, a few studies have explored alternative meta-heuristics, such as bacterial foraging optimization algorithm (BFOA) [13], invasive weed optimization (IWO) [14], artificial rabbit optimization (ARO) [15] for both optimal location and size estimation. These algorithms offer flexibility to optimize for single or multiple DGs with single- or multi-objective (SO or MO) approaches. However, like their counterparts, these methods often rely on sensitivity approaches for DG placement.

In contemporary research, there has been a growing advocacy for hybridizing analytical methods with meta-heuristic techniques that offer enhanced optimization capabilities. For instance, LSF based BSOA [9], improved analytic PSO (IA-PSO) [16], LSF based chaotic WOA (LSF-CWOA) [17] have been proposed. These hybrid methods leverage the sensitivity approach to determine the optimal DG locations, while employing a meta-heuristic approach for sizing. However, it is important to note that sensitivity approaches often rely on linear approximations of the system constraints, which may not accurately capture the non-linear behavior inherent in distribution networks, thereby leading to suboptimal results and poor optimization outcomes.

In response to these challenges, researchers have increasingly turned toward hybrid meta-heuristic approaches that combine two or more meta-heuristic algorithms. Examples of such approaches include ACO-ABC [5], harmony search based particle ABC (HAS-PABC) [18], ABC with cuckoo search (ABC-CS) [19], EHO-PSO [20], ABC with bat algorithm (ABC-BAT), ABC with cat swarm optimization (ABC-CSO) [6], arithmetic optimization algorithm with slap swarm algorithm (AOASSA) [21]. One of the limitations of this hybridization has increased computational burden.

Moreover, significant efforts have been directed towards refining and enhancing standard meta-heuristic approaches to address the challenges posed by DG placement and sizing optimization. These efforts include developments such as swine influenza model based optimization (QOSIMBO-Q) [22], multi-objective Taguchi approach (MOTA) [23], quasi-oppositional TLBO (QOTLBO) [24], comprehensive TLBO (CTLBO) [25], hybrid TLBO (HTLBO) [26], NSGA-II with fuzzy decision-making tool (NSGA-II/FDMT) [27], multi-objective chaotic SCA (MO-CSCA) [28], enhanced search group (ESGA) [29], jellyfish search (LJS) [30], improved golden jackal optimization (IGJO) [31], have been proposed to tackle the complexities of multi-objective optimization in DG placement and sizing.

Despite the advancements in optimization techniques, the field faces ongoing challenges related to scalability, accuracy, and robustness in addressing the complex optimization problem posed by DG placement and sizing in distribution networks. To address these challenges, this article proposes a multi-objective CPSOS (MO-CPSOS) method for optimal DG placement and sizing using Pareto frontier approach. Tian et.al., originally proposed the CPSOS approach [32]. Inspired by the success of PSO, the CPSOS approach introduces a chaotic map that aims to improve diversity and prevents premature convergence. Additionally, a sigmoid-based acceleration coefficient strategy to enhance diversity and convergence accuracy. However, the application of MO-CPSOS has not been found in the optimal DG placement and sizing. A wide range of factors, including technical and economic aspects can impact optimal DG placement and sizing. However, the current model focuses on three technical factors to benchmark against a common standard and establish a clear comparison with existing algorithms. This article provides scope for further investigation.

The novelty of this paper is as follows:

- Multi-objective approach using Pareto frontier method with objectives: power loss, voltage deviation and voltage stability, to ensure a solution that is both balanced and comprehensive.
- Adaptive adjustment of social and cognitive acceleration coefficients, ensuring flexibility and adaptability.
- Easy algorithm implementation and scalability to larger networks.
- Simulations performed on IEEE networks like 33-bus, 69-bus, and 118-bus systems.

The rest of the article is organized as follows: in Section-II the proposed multi-objective modeling is depicted, and in Section-III the proposed approach CPSOS is presented. While Section-IV describes test systems and test cases and Section-V illustrates results and discussions. Finally, in Section-VI conclusions are outlined.

II. Multi-Objective Function Modeling

A. Modeling of Distribution Line

A simple balanced distribution line is shown in Fig.1, connected between *bus-j* and *bus-k*. The real and reactive power flows are respectively, given in (1-2):

$$P_{jk} = V_j \sum_{k=1}^{N} V_k \left[G_{jk} \cos\left(\delta_j - \delta_k\right) + B_{jk} \sin\left(\delta_j - \delta_k\right) \right] \tag{1}$$

$$Q_{jk} = V_j \sum_{k=1}^{N} V_m \left[G_{jk} \sin\left(\delta_j - \delta_k\right) - B_{jk} \cos\left(\delta_j - \delta_k\right) \right] \tag{2}$$

where, V_j and V_k are voltages at respective *buses j* and *k*. This model is used to compute various parameters of the DN.

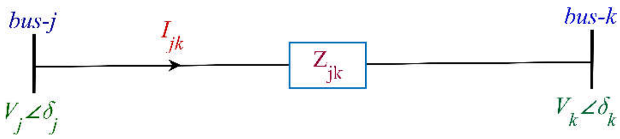

Fig.1. Load flow model of the distribution line.

B. Formulation of Multi-Objective Optimization

Consider $f_i(x)$ be the i^{th} *objective function* (OF) where $x = (x_1, x_2, x_3, \ldots, x_N)$ is a set of decision vectors from a feasible space. The mathematical representation of multi-objective function for M objectives is given by (3) [33]:

$$\min\left\{f_1(x), f_2(x), \ldots, f_M(x)\right\}, \forall x \quad (3)$$

The best compromised solution can be obtained by the principle of non-dominating sorting. A decision vector x_1 is said to dominate x_2, if and only if:

$$\forall i : f_i(x_1) \le f_i(x_2), \quad i = 1,2,\ldots,N \quad (4)$$

$$\exists i \mid f_i(x_1) < f_i(x_2), \quad i = 1,2,\ldots,N \quad (5)$$

This means, if x_1 is not inferior to solution x_2 in all objectives, x_1 is firmly superior to x_2 in at least one objective. Further, with the help of fuzzy set theory, the best compromised solution is obtained from the Pareto front. In this work three *OFs* namely, (i) minimizing real power loss, (ii) maximizing voltage stability, and (iii) alleviating voltage deviation is considered as a MO approach to obtain optimal placement and size of DG. The detailed formulation of *OFs* is given below:

B.1. Components of Multi-Objective Function

1) Minimizing Real Power Loss Index (RPLI)

The objective OF_{RPLI} given by (6) is to reduce real power loss, where $P_{loss\_with\_dg}$ and P_{base_loss} is TRPL with and without DG, respectively, while P_{loss} is given by (7), where P_j and P_k are active power, while Q_j and Q_k reactive power injections respectively at *bus-j* and *bus-k;* r_{jk} is element of bus impedance; N is the bus number.

$$OF_{RPLI} = \min\left(\frac{P_{loss\_with\_dg}}{P_{base\_loss}}\right) \quad (6)$$

$$P_{loss} = \frac{r_{jk}}{V_j V_k}\sum_{j=1}^{N}\sum_{k=1}^{N}\left[\left(P_j P_k + Q_j Q_k\right)cos\left(\delta_j - \delta_k\right) + \left(Q_j P_k + P_j Q_k\right)sin\left(\delta_j - \delta_k\right)\right] \quad (7)$$

2) Improving System Voltage Stability Index (SVSI)

The objective OF_{SVSI} given by (8) is to improve system voltage stability. SVSI can measure the level of stability of the distribution network [34]. OF_{SVSI} close to unity gives the perfect voltage stability. Here VSI_k is given by (9),

$$OF_{SVSI} = \min\left(\frac{1}{VSI_k}\right) \quad \text{(or)} \quad \max\left(VSI_k\right) \quad (8)$$

$$VSI_k = V_k^4 - 4\times\left(P_j x_{jk} - Q_j r_{jk}\right)^2 - 4\times\left(P_j r_{jk} - Q_j x_{jk}\right)^2 V_k^2 \quad (9)$$

3) Mitigating System Voltage Deviation Index (SVDI)

The objective (OF_{SVDI}) given in (10) is to mitigate system voltage deviation. This ensures better voltage quality for the consumers. The value (OF_{SVDI}) near to zero implies of reduced voltage deviation.

$$OF_{SVDI} = \min\left(\sum_{j=1}^{N}\left(V_j - V_{rated}\right)\right) \quad (10)$$

B.2. The Optimization of Objective Function

In this work following objectives are considered:

i) Single-objective (SO) Function: only OF_{RPLI} is considered.

$$OF_1 = min\left(OF_{RPLI}\right) \quad (11)$$

ii) Multi-objective (MO) Function: Three objectives OF_{RPLI}, OF_{SVDI}, and OF_{SVSI} considered. A Pareto frontier approach is used to obtain optimal solution.

$$OF_2 = \min\left(OF_{RPLI},\ OF_{SVDI},\ OF_{SVSI}\right) \quad (12)$$

C. Equality and Inequality Constraints

The real and reactive power balances at *bus-j* are given by (13) and (14) respectively.

$$P_j = V_j \sum_{k=1}^{N} V_k Y_{jk} \cos\left(\phi_{jk} + \delta_k - \delta_j\right) \quad (13)$$

$$Q_j = V_j \sum_{k=1}^{N} V_k Y_{jk} \sin\left(\phi_{jk} + \delta_k - \delta_j\right) \quad (14)$$

Slack bus voltage and angle,

$$V_1 = 1.00\,pu \text{ and } \delta_1 = 0.0 \ \ radians \quad (15)$$

Maximum limit of power injected by DGs, given by (16).

$$\sum_{j=1}^{N} P_{dg,j} + P_{total\_loss} \le \sum_{j=1}^{N} P_{demand,j} \quad (16)$$

The DG size is calculated such that voltage magnitude at *bus-j* should be within limits, given by (17)

$$0.95 \le V_j \le 1.05 \quad (17)$$

Capacity limits of the feeder,

$$0 \le I_{jk} \le I_{jk}^{Max} \quad (18)$$

III. The Proposed Approach: Chaotic PSO with Sigmoid Function

A. Standard PSO Approach:

The foraging behaviors of animals inspired the PSO approach. Each particle in this approach has a velocity and position represented by vectors, and these particles also have an individual or local best (p_{best}). These vectors denoted as $v_{ij} = (v_{i1}, v_{i2}, v_{i3} \ldots v_{ij})$ and $x_{ij} = (x_{i1}, x_{i2}, x_{i3} \ldots x_{ij})$ respectively, where j is the dimension, help update the particle's velocity and position using (19) and (20). In these equations, ω inertia weight, c_1 is cognition parameter, while c_2 is the social parameter, and r_1 and r_2 are random numbers in between 0 and 1.

$$v_{ij}^{\tau+1} = \omega \times v_{ij}^{\tau} + c_1 \times r_1 \times \left(p_{best,ij} - x_{jk}^{\tau}\right) + c_2 \times r_2 \times \left(g_{best,j} - x_{ij}^{\tau}\right) \quad (19)$$

$$x_{ij}^{\tau+1} = x_{ij}^{\tau} + v_{ij}^{\tau+1} \quad (20)$$

B. Chaotic PSO Approach

In PSO approach, particle initialization can influence convergence. The Chaotic PSO method uses a sequence-based initialization to add diversity to the particles. A chaotic logistic map is first utilized to generate initial positions using (21), where y_i represents (i^{th}) chaotic variable, bifurcation coefficient (α), population (N), while dimension D (number of DGs in this study). The search space is mapped by generated chaotic variables using (22):

$$y_{ij}^{\tau+1} = \alpha \times y_{ij}^{\tau} \times \left(1 - y_{ij}^{\tau}\right), \quad i = 1,2,3,...,N; j = 1,2,...,D \tag{21}$$

$$x_{ij}^{\tau} = x_{\min,j} + y_{ij}^{\tau} \times \left(x_{\max,j} - x_{\min,j}\right) \tag{22}$$

C. Acceleration Coefficients based on Sigmoid Function:

In PSO, the movement of particles towards their p_{best} and g_{best} depend on the values of c_1, c_2, and ω. Properly selecting these parameters is crucial for achieving an optimal global solution. The adaptiveness of the solution at optimum depends on how well these control parameters are adopted [32]. This section elaborates in detail the later considerations of choosing acceleration coefficients and its impact on the convergence of PSO.

Typically, many studies have opted for equal coefficient values ($c_1 = c_2$), but this method may limit particle movement confined to the midpoint between p_{best} and g_{best}, as depicted in Fig.2 (a). In contrast, unequal coefficients drive solutions toward either p_{best} or g_{best}, based on the relative values of c_1 and c_2. The particle moves toward p_{best} if value of $c_1 > c_2$ (Fig.2 (b)), consequently, towards g_{best} if $c_1 < c_2$ (Fig.2 (c)). To expedite convergence, c_2 should exceed c_1, ensuring that the new particle position is in closer proximity to g_{best}. To have a smoother transition to non-linear state a sigmoid function is introduced, where cognitive (c_p) and social (c_g) parameters change according to (23) and (24).

$$c_p^{\tau} = \left(c_f - c_i\right) \times \left(\frac{\tau}{\tau_{\max}} - 1\right)^2 + \left(\frac{1}{1 + e^{-\lambda\left(\tau/\tau_{\max}\right)}}\right) \tag{23}$$

$$c_g^{\tau} = \left(c_f - c_i\right) \times \left(\frac{\tau}{\tau_{\max}}\right)^2 + \left(\frac{1}{1 + e^{-\lambda\left(\tau/\tau_{\max}\right)}}\right) \tag{24}$$

The initial and final values of c_i and c_f help maintain balance in the particle movements, when $\lambda = 0.0001$, ranges vary $0.5 < c_p <$ 2.5 and $2.5 < c_g < 0.5$ as depicted in Fig.3. Similar approach is used to obtain Time-Varying Adaptive Acceleration Coefficients (TVAC) [35]. This adaptive approach enables the particles to explore different areas of the search space. The formula for updating velocity with acceleration coefficients using sigmoid function is modified as (25), where are τ is current and τ_{max} maximum iterations. Update of inertia weight is outlined in (26), where ω_{max} (0.9) is initial and ω_{min} (0.4) is final values of the inertia weight.

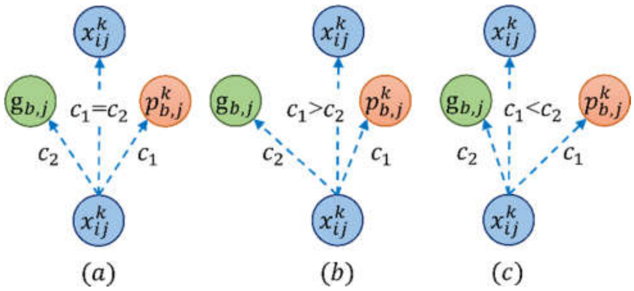

Fig.2. Effect of cognitive and social accelerating parameters on particle movement.

$$v_{ij}^{\tau+1} = \omega^{\tau} \times v_{ij}^{\tau} + c_p \times r_1 \times \left(p_{best,ij}^{\tau} - x_{jk}^{\tau}\right) + c_g \times r_2 \times \left(g_{best,j} - x_{ij}^{\tau}\right) \tag{25}$$

$$\omega^{\tau} = \left(\omega_{\max} - \omega_{\min}\right) \times \left(1 - \frac{\tau}{\tau_{\max}}\right) + \omega_{\min} \tag{26}$$

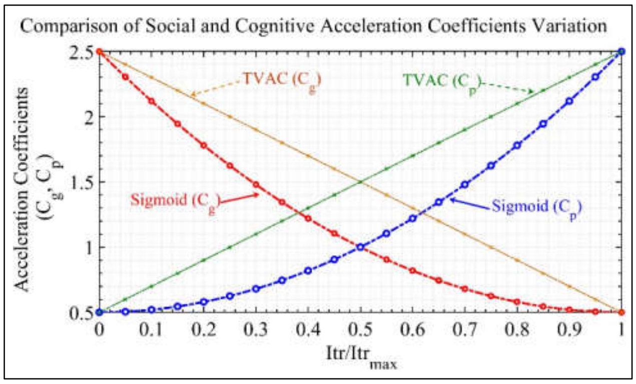

Fig.3. Variations of acceleration coefficients using proposed sigmoid-function and TVAC.

D. CPSOS Approach: Update Mechanism

In the early stages of the algorithm, a regular varying function $x^{\delta}l(x)$ is introduced to speed up exploration into (27). Later, to prevent trapping into local optima, $l(x)$ a slowly varying function is applied as in (28). In this later stage, when the swarm average surpassed by a particle's fitness, a Gaussian mutation is used helping enhance the search capability, as outlined in (29) and (30). In (27), δ is control parameter, and in (29) and (30) $gaussian_j()$ is Gaussian distribution generated random number.

Fig.4 illustrates the flowchart of proposed CPSOS strategy.

$$x_{ij}^{\tau+1} = x_{ij}^{\tau} + v_{ij}^{\tau+1} + x^{\delta} l(x) \tag{27}$$

$$x_{ij}^{\tau+1} = x_{ij}^{\tau} + v_{ij}^{\tau+1} + l(x) \tag{28}$$

$$p'_{best,ij} = p_{best,ij} + gaussian_j() \tag{29}$$

$$g'_{best,ij} = g_{best,ij} + gaussian_j() \tag{30}$$

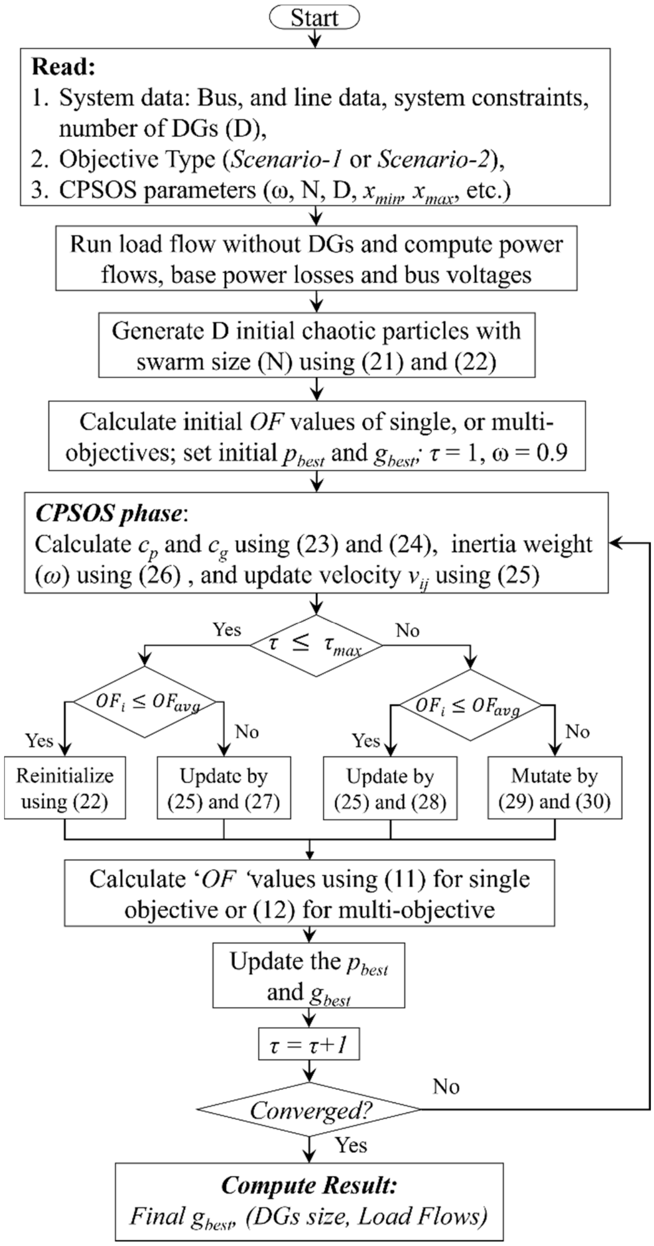

Fig.4. Strategy of optimal placement and sizing of DGs using proposed MO-CPSOS.

IV. Test Systems and Test Cases

The test systems to assess the proposed approach are described in Table I:

TABLE I

Test Systems Considered in this Study

S. No.	IEEE System	Power Demand		Power Loss	
		Active (kW)	Reactive (kVAr)	Active (kW)	Reactive (kVAr)
1	33-Bus	3710	2300	210.846	135.14
2	69-Bus	3792	2694	224.948	102.14
3	118-Bus	22709.72	17041.07	1296.57	978.06

The parameters considered in this simulation are in Table II. The following two scenarios were considered to evaluate the sturdiness of the proposed method:

Scenario-1: *Single-Objective (SO) optimization* using (11)
Scenario-2: *Multi-Objective (MO) optimization* using (12)

The following cases for DG placement with unity power factor (UPF) were tested for both scenario:

Case-1: Single DG placement.
Case-2: Three DGs placement.
Case-3: Seven DGs placement.

TABLE II

Parameters Considered in Simulation

Method	Population Size	c_1 or c_p	c_2 or c_g	Maximum Iterations	No. of Trails
Proposed CPSOS/ MO-CPSOS	15	2.5 to 0.5	0.5 to 2.5	100	250
TVAC-PSO	15	2.5 to 0.5	0.5 to 2.5	100	250
PSO	15	1.5	1.5	100	-

V. Results and Discussions

A. Evaluation of CPSOS Performance: Scenario-1

The robustness and efficiency of the proposed CPSOS technique within a SO framework (*Scenario-1*) is analyzed in this section, which focuses on minimizing the real power loss index (RPLI) using (11). The simulation results are benchmarked against well-established optimization approaches using test cases: integration of DG with *Case-1*, and *Case-2* on 33-bus, 69-bus, and with *Case-3* on the 118-bus system.

Case-1: Table III (33-bus system) demonstrates the efficiency of the CPSOS approach, achieving a slightly higher percentage TRPL reduction (47.407%) compared to DE (47.406%). Importantly, CPSOS attains this with a smaller installed DG capacity (2589.96 kW compared to DE's 2590 kW). Methods such as LSF-BSOA, PSO, IA-PSO, and HAS-PABC exhibited higher losses. Similar results are observed on the 69-bus system (Table-IV). CPSOS achieves a 63.03% TRPL reduction and an optimal DG size of 1872.66 kW. While NSGAII/FDMT and AOASSA approaches show comparable performance in terms of TRPL reduction and optimal DG size, CPSOS maintains a slight advantage. Fig. 5 and Fig. 6 clearly illustrate the superior convergence speed of CPSOS compared to TVAC-PSO and PSO for both the 33-bus and 69-bus systems.

TABLE III

Comparison using Case-1 of Scenario-1 (33-Bus DN)

	LSF-BSOA [9]	PSO [5]	IA-PSO [16]	HAS-PABC [18]	DE [4]	**CPSOS**
Base Loss (kW)	210.84	211	211	211	210.84	210.846
TRPL (kW)	118.12	115.29	111.17	111.03	110.89	**110.89**
% TRPL Reduction	43.98	44.36	47.313	47.379	47.406	**47.407**
DG Size (kW)	1857.5	3150	2490	2598	2590	**2589.96**
Location	6	6	6	6	6	6

TABLE IV

COMPARISON USING CASE-1 OF SCENARIO-1 (69-BUS DN)

	ABC-CS-LSF [19]	LSF-CWOA [17]	IGJO [31]	NSGAII/FDMT [27]	AOASSA [21]	**CPSOS**
Base Loss (kW)	224.948	224.99	225.00	225	225	224.948
TRPL (kW)	83.21	83.22	83.223	83.22	83.22	**83.17**
% TRPL Reduction	63.009	63.012	63.012	63.013	63.013	**63.03**
DG Size (kW)	1870	1872.7	1872.7	1872.6	1872.7	**1872.66**
Location	61	61	61	61	61	61

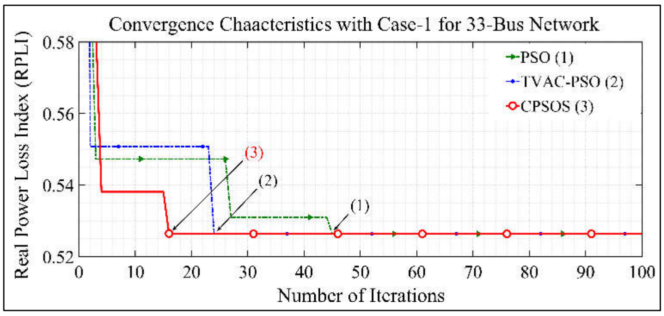

Fig.5. Comparison of convergence characteristics on 33-bus using *Case-1* of *Scenario-1*

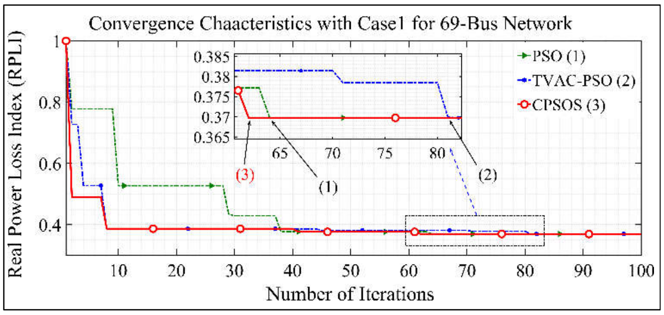

Fig.6. Comparison of convergence characteristics on 69-bus using *Case-1* of *Scenario-1*

Case-2: On the 33-bus system (Table V), CPSOS, LJS, and CBOM demonstrate the highest TRPL (65.50%), surpassing HAS-PABC (65.49%) and IAT (61.657%). Importantly, CPSOS achieves this with the smallest optimal DG capacity (2933.58 kW), compared to LJS (2946.71 kW) and CBOM (2946.66 kW). Fig.7 confirms CPSOS's superior convergence speed and ability to avoid the convergence issues compared to TVAC-PSO and PSO. Similar results are seen on 69-bus network (Table VI). CPSOS secures a 69.153% TRPL reduction, outperforming IGJO (69.144%), CBOM (69.143%), AOASSA (69.142%) and ACO-ABC (69.14%). Fig.8 showcases the significantly faster and more reliable convergence of CPSOS compared to TVAC-PSO. Notably, PSO fails to escape local optima.

TABLE V

COMPARISON USING CASE-2 OF SCENARIO-1 (33-BUS DN)

		IAT [36]	HAS-PABC [18]	CBOM [7]	LJS [30]	**CPSOS**
Base Loss (kW)		210.99	211	210.99	210.98	210.846
TRPL (kW)		80.9	72.81	72.787	72.78	72.75
% TRPL Reduction		61.657	65.49	65.50	65.50	**65.50**
DG Size (kW)	DG-1	1312	755	801.706	801.8	771.53
	2	462	1168	1091.33	1091.31	1096.79
	3	657	1073	1053.64	1053.6	1065.54
	Total	2431	2996	2946.66	2946.71	**2933.86**
Location		6, 18, 32	14, 24, 30	13, 24, 30	13, 24, 30	13, 24, 30

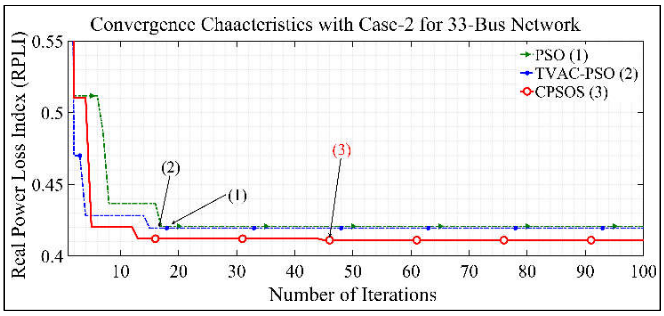

Fig.7. Convergence characteristics comparison using *Case-2* of *Scenario-1* on 33-bus.

TABLE VI

COMPARISON USING CASE-2 OF SCENARIO-1 (69-BUS DN)

		ACO-ABC[6]	AOASSA [21]	CBOM [7]	IGJO [31]	**CPSOS**
Base Loss (kW)		225	225	225	225	224.948
TRPL (kW)		69.43	69.43	69.428	69.427	**69.398**
% TRPL Reduction		69.14	69.142	69.143	69.144	**69.153**
DG Size (kW)	DG-1	559.7	526.84	527	526.668	526.67
	2	346.8	380.35	380	380.51	380.21
	3	1715.9	1718.9	1719	1718.97	1718.97
	Total	2622.4	2626.09	2526	2626.148	**2625.84**
Location		11, 21, 61	11, 18, 61	11, 18, 61	11, 18, 61	11, 17, 61

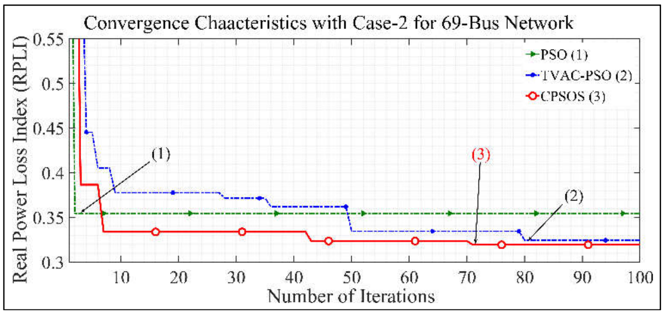

Fig.8. Convergence characteristics comparison using *Case-2* of *Scenario-1* on 69-bus.

Case-3: On the extensive IEEE 118-bus network (Table VII), the proposed CPSOS method demonstrates superior performance with a 60.28% TRPL reduction. This exceeds the results achieved by NHM (60.27%), ESGA (60.239%), CTLBO (60.23%), and IGJO (60.218%). Fig.9 further illustrates CPSOS's rapid convergence and attainment of optimal solution, whereas TVAC-PSO and PSO exhibit slower convergence and fail to reach the same level of optimization.

TABLE VII
COMPARISON USING CASE-3 OF SCENARIO-1 (IEEE 118-BUS)

		IGJO [31]	CTLBO [25]	ESGA [29]	NHM [37]	CPSOS
Base Loss (kW)		1298.09	1298.019	1298.092	1298	1296.57
TRPL (kW)		516.407	516.256	516.128	515.7	515.004
% TRPL Reduction		60.218	60.23	60.239	60.27	**60.28**
DG Size (MW)	DG-1	1.7949	1.8176	3.7082	1.802	1.8176
	2	1.8332	1.2764	1.1545	1.267	1.2764
	3	2.7346	2.7671	2.3337	2.371	2.7646
	4	2.4168	2.5333	2.5333	2.287	2.5333
	5	2.1062	2.0949	2.0949	2.080	2.0949
	6	1.0876	1.6631	1.6631	1.667	1.6631
	7	3.1198	3.1189	3.1189	2.780	3.1199
	Total	15.0931	15.2713	16.6066	14.614	**15.2698**
Location		32, 39, 47, 72, 85, 91, 109	20, 44, 52, 75, 83, 100, 114	30, 42, 50, 72, 80, 96, 109	32, 39, 47, 72, 85, 91, 109	20, 44, 52, 75, 83, 100, 115

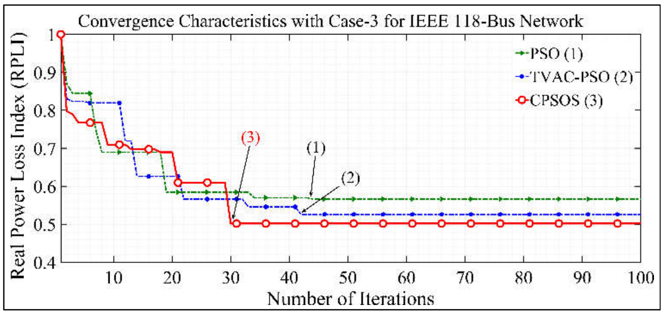

Fig.9. Comparison of convergence characteristics on 118-bus using *Case-3* of *Scenario-1*

Table VIII depicts statistical data from 250 trials of the proposed CPSOS under *Scenario-1* (single-objective optimization). Results consistently demonstrate superior efficiency of CPSOS compared to other approaches. In all cases (with one, and three DGs across 33-bus, 69-bus, and seven DGs on 118-bus systems), proposed CPSOS approach achieved the highest total real power loss (TRPL) reduction. The proposed multi-objective approach performance is examined in the following section.

TABLE VIII
STATISTICAL RESULTS DATA AFTER 250 TRIALS

Test System	Case	Best PLI	Worst PLI	Average PLI	SD PLI	Average CPU Tim (in m. s.)
33-Bus System	1	0.52597	0.53223	0.52602	0.00049	7.4966
	2	0.34508	0.41673	0.35787	0.00998	7.8270
69-Bus System	1	0.36982	0.42936	0.38524	0.06392	24.8556
	2	0.30850	0.35261	0.32395	0.08856	25.0838
118-Bus System	3	0.39720	0.47887	0.44033	0.01292	76.8830

B. Study of MO-CPSOS Performance: Scenario-2

The superiority of the proposed MO-CPSOS approach using *Scenario-2 is* evaluated in this section which considers three objectives: minimizing RPLI, maximizing SVSI, and mitigating SVDI as mentioned in objective function OF_2 in (12). Results are compared to well-known methods such as ARO [15], EHO-PSO [20], QOSIMBO-Q [22], MOTA [23], CTLBO, CTLBO-ε [44], MO-CSCA [28], and ESGA [29], all which use similar three-objective optimization approach in *Scenario-2*.

33-bus test system: Table IX reveals that the proposed MO-CPSOS approach achieves a performance similar to CTLBO in terms of TRPL reduction (59.261%, and 59.26%), voltage deviation index (SVDI is 0.0026), and voltage stability index (SVSI is 0.9481), Crucially, MO-CPSOS attains this with smaller optimal DG size (3718.45 kW) compared to CTLBO (3721.1 kW). While ESGA and ARO show better loss reduction (63.485% and 63.508%), they fall short in optimizing SVDI and VSI. Fig.10 clearly illustrates the voltage profile improvement achieved by MO-CPSOS compared to ESGA and Aro methods. Note that both CTLBO and CTLBO-ε (ε-constraint method) result in voltage profiles exceeding 1 p.u. Fig.11 demonstrates the superiority of the proposed approach showcasing the Pareto Optimal Front (POF) over TVAC-PSO using *Scenario-2*.

TABLE IX
COMPARISON USING CASE-2 OF SCENARIO-2 (33-BUS DN)

		CTLBO-ε [25]	ESGA [29]	ARO [15]	CTLBO [25]	MO-CPSOS
Base Loss (kW)		210.99	210.998	210.98	210.99	210.846
TRPL (kW)		96.17	77.042	76.99	85.959	85.897
% TRPL Reduction		54.42	63.487	63.508	59.26	**59.261**
DG Size (kW)	DG-1	1182.6	956.4	956.6	1036.4	1035.6
	2	870.6	1131	1129.2	1163.0	1159.53
	3	1629.6	1293.5	1291.3	1521.7	1523.32
	Total	3692.8	3380.9	3377.1	3721.1	**3718.45**
RPLI		0.4558	0.3651	0.3649	0.4074	**0.4074**
SVDI		0.0009	0.0065	0.0065	0.0026	**0.0026**
SVSI		0.9638	0.91676	0.9183	0.9481	**0.9481**
Location		13, 25, 30	13, 24, 30	13, 24, 30	13, 24, 30	13, 24, 30

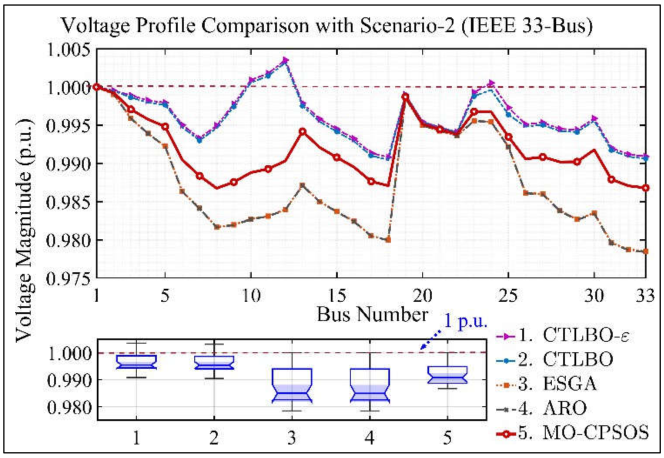

Fig.10. Voltage profiles comparison on *33-bus* (*Scenario-2* with *Case-2*).

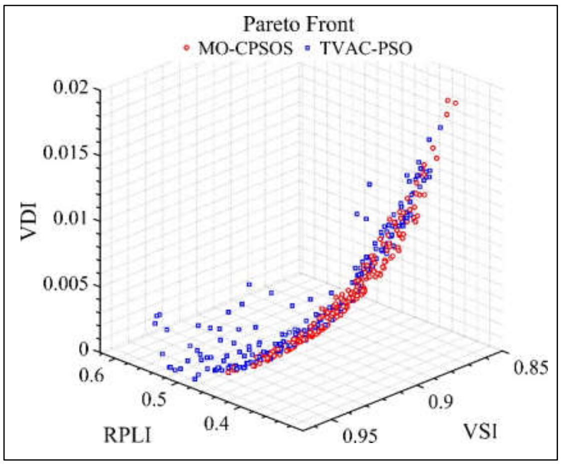

Fig.11. Pareto Optimal Front of MO-CPSOS and TVAC-PSO on IEEE 33-Bus System using *Scenario-2* with *Case-2*.

69-bus test system: Table X demonstrates the superior power loss reduction of the proposed MO-CPSOS approach (64.95%) compared to MO-CSCA (64.58%), CTLBO-ε (64.57%) and QOSIMBO-Q (64.56%). Moreover, MO-CPSOS achieves the best system voltage deviation index (SVDI) of 0.00028, outperforming MO-CSCA and CTLBO-ε (both at 0.0003). In terms of SVSI, MO-CPSOS also excels with a value of 0.97705, surpassing CTLBO-ε (0.9770) and QOSIMBO-Q (0.9768). While ESGA shows higher TRPL reduction (67.942%), it fails to optimize SVDI and SVSI, resulting in a suboptimal voltage profile (Fig.12). The proposed MO-CPSOS demonstrates a clear improvement in voltage profile compared to other methods. Fig.13 illustrates the MO-CPSOS approach's advantage over TVAC-PSO when considering the multi-objective POF.

TABLE X

COMPARISON USING CASE-2 OF SCENARIO-2 (69-BUS DN)

		QOSIMBO-Q [22]	CTLBO-ε [25]	ESGA [29]	MO-CSCA [28]	**MO-CPSOS**
Base Loss (kW)		224.9	224.9	224.9917	224.95	224.948
TRPL (kW)		79.7	79.660	72.127	79.69	**78.8381**
% TRPL Reduction		64.56	64.58	67.942	64.57	**64.95**
DG Size (kW)	DG-1	775.4	965.8	642.6	453.12	449.42
	2	1438.5	230.7	419.6	2190.7	2112.45
	3	723.5	2133.6	1194.7	676.3	806.61
	Total	2937.4	3330.1	2256.94	3320.1	3368.47
RPLI		0.3544	0.3542	0.3206	0.3543	**0.35047**
SVDI		0.0007	0.0003	0.0016	0.0003	**0.00028**
SVSI		0.9768	0.9770	0.95166	0.9798	0.97705
Location		15, 61, 63	12, 25, 61	11, 21, 61	21, 61, 67	21, 61, 67

118-bus test system: Table XI highlights the superiority of the proposed MO-CPSOS approach. It achieves the highest percentage TRPL reduction (56.846%), outperforming EHO-PSO (56.82%) and MOTA (52.38). Additionally, MO-CPSOS secures the best SVDI (0.02803) and SVSI (0.8930), surpassing EHO-PSO and MOTA. While ARO and ESGA exhibit slightly higher TRPL reductions, they compromise on optimal SVDI and SVSI. Importantly, MO-CPSOS achieves the most efficient solution with total optimal DG size of 18.9577 MW. Fig.14 visually confirms the significant voltage profile improvement attained by MO-CPSOS. Furthermore, Fig.15 depicts a superior POF compared to TVAC-PSO when simultaneously minimizing RPLI and SVDI while maximizing SVSI.

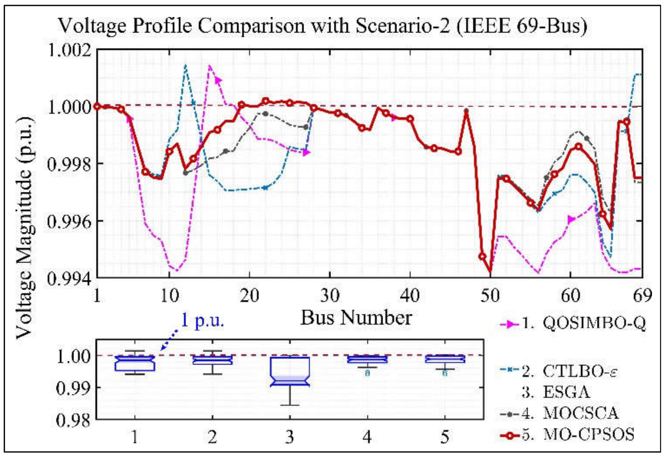

Fig.12. Voltage profiles comparison on *69-bus* (*Scenario-2* with *Case-2*).

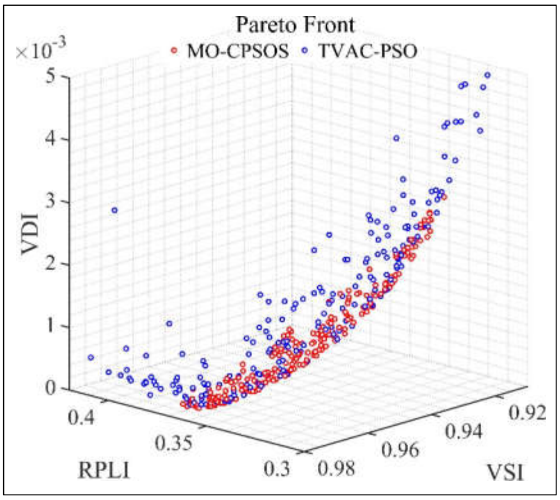

Fig.13 Pareto Optimal Front of MO-CPSOS and TVAC-PSO on IEEE 69-Bus System using *Scenario-2* with *Case-2*.

TABLE XI

COMPARISON USING CASE-3 OF SCENARIO-2 (IEEE 118-BUS)

		MOTA [23]	ARO [15]	ESGA [29]	EHO-PSO [20]	**MO-CPSOS**
Base Loss (kW)		1298.1	1298.09	1298.091	1296.3	1296.57
TRPL (kW)		618.2	548.455	548.933	559.7	**559.5158**
% TRPL Reduction		52.38	57.749	57.712	56.82	**56.846**
DG Size (MW)	DG-1	1.92	2.1308	2.1369	3.852	1.9387
	2	4.38	3.8884	1.4575	1.716	1.5640
	3	2.28	1.4482	3.8929	3.679	3.9102

	4	1.38	2.8365	2.838	2.708	3.2507
	5	2.88	1.9786	2.4602	2.456	2.6448
	6	1.92	2.4644	1.9728	1.875	2.0375
	7	3.60	3.5005	3.4999	3.259	3.6118
	Total	18.36	18.2474	18.5282	19.545	**18.9577**
RPLI		0.4762	0.4225	0.4229	0.4318	**0.4315**
SVDI		0.0305	0.0309	0.0309	0.0348	**0.02803**
SVSI		0.8797	0.8865	0.7825	0.8910	**0.8930**
Location		3, 42, 60, 2, 78, 92, 108	20, 39, 48, 73, 85, 91, 109	20, 42, 50, 73, 80, 96, 109	18, 42, 50, 74, 79, 91, 109	20, 44, 52, 74, 83, 100, 114

The proposed MO-CPSOS approach demonstrated superior performance and efficacy through optimal DG placement and sizing thereby reducing real power loss and voltage deviation, while enhancing voltage stability. Its robustness is validated across IEEE 33-bus, 69-bus, and extensive IEEE 118-bus test systems.

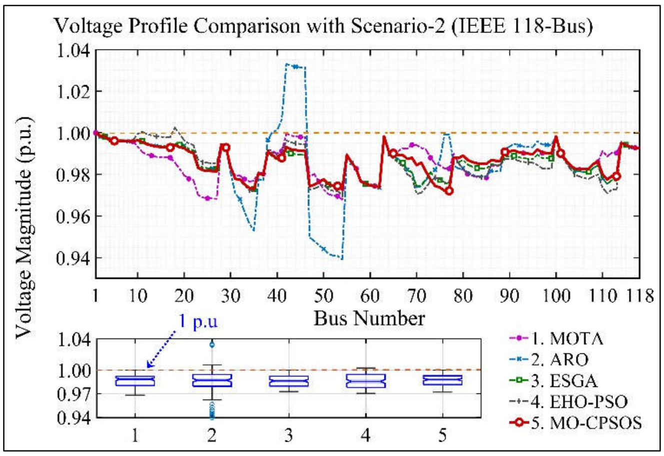

Fig.14. Voltage profile comparisons on *118-bus* (*Scenario-2* with *Case-3*).

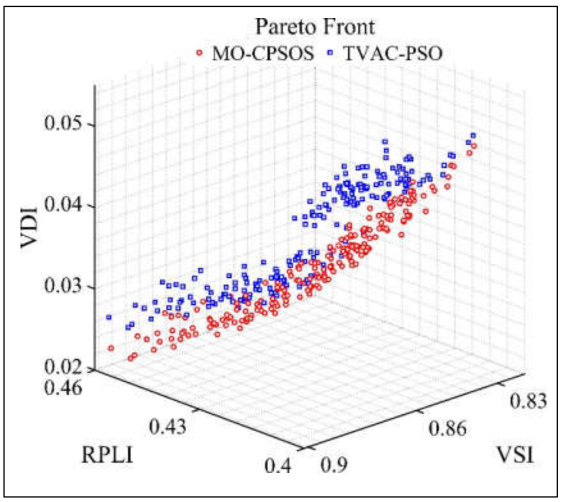

Fig.15. Pareto Optimal Front of MO-CPSOS and TVAC-PSO on IEEE 118-Bus System using *Scenario-2* with *Case-3*

VI. CONCLUSIONS

The multi-objective chaotic particle swarm optimization with sigmoid-based acceleration coefficients (MO-CPSOS) algorithm provides an effective and efficient solution for optimizing the placement and sizing of distributed generators (DGs) within distribution networks (DNs). Through extensive simulations on the IEEE 33-bus, 69-bus, and larger 118-bus systems, the MO-CPSOS approach has demonstrated its efficacy in both single-objective and multi-objective optimization contexts. In single-objective problems, the CPSOS algorithm consistently outperformed existing methods in reducing real power loss, determining optimal DG sizes, and improving convergence speed. Additionally, the algorithm exhibited superior convergence characteristics with higher accuracy. In multi-objective optimization, the MO-CPSOS approach, using Pareto optimality, achieved competitive results by reducing power loss, minimizing voltage deviation, and improving voltage stability compared to other methods. The algorithm's ability to optimize multiple conflicting objectives ensures a balanced, and comprehensive solution that addresses the complex challenges of DG placement and sizing in distribution networks. Overall, the proposed MO-CPSOS algorithm offers a promising framework for achieving optimal placement and sizing of DG while supporting the efficient and sustainable operation of distribution networks amidst the increasing penetration of renewable energy sources.

REFERENCES

[1] T. Lu, P. Sherman, X. Chen, S. Chen, X. Lu, and M. McElroy, "India's potential for integrating solar and on- and offshore wind power into its energy system," *Nat Commun*, vol. 11, no. 1, Dec. 2020, doi: 10.1038/s41467-020-18318-7.

[2] P. C. Chen *et al.*, "Analysis of voltage profile problems due to the penetration of distributed generation in low-voltage secondary distribution networks," *IEEE Transactions on Power Delivery*, vol. 27, no. 4, pp. 2020–2028, 2012, doi: 10.1109/TPWRD.2012.2209684.

[3] R. K. Singh and S. K. Goswami, "Multi-objective optimization of distributed generation planning using impact indices and trade-off technique," *Electric Power Components and Systems*, vol. 39, no. 11, pp. 1175–1190, Jan. 2011, doi: 10.1080/15325008.2011.559189.

[4] Israfil Hussain and Anjan Kumar Roy, "Optimal Size and Location of Distributed Generations using Differential Evolution (DE)," in *IEEE 2nd National Conference on Computational Intelligence and Signal Processing (CISP)* , IEEE, 2012, pp. 57–61.

[5] S. Kansal, V. Kumar, and B. Tyagi, "Optimal placement of different type of DG sources in distribution networks," *International Journal of Electrical Power and Energy Systems*, vol. 53, no. 1, pp. 752–760, 2013, doi: 10.1016/j.ijepes.2013.05.040.

[6] R. Palanisamy and S. K. Muthusamy, "Optimal Siting and Sizing of Multiple Distributed Generation Units in Radial Distribution System Using Ant Lion Optimization Algorithm," *Journal of Electrical Engineering and Technology*, vol. 16, no. 1, pp. 79–89, Jan. 2021, doi: 10.1007/s42835-020-00569-5.

[7] G. Memarzadeh, M. Arabzadeh, and F. Keynia, "A new optimal allocation of DGs in distribution networks by using coot bird optimization method," *Energy Informatics*, vol. 6, no. 1, Dec. 2023, doi: 10.1186/s42162-023-00296-x.

[8] H. Van Tran, A. V. Truong, T. M. Phan, and T. T. Nguyen, "Optimal placement and operation of soft open points, capacitors, and renewable distributed generators in distribution power networks to reduce total one-year energy loss," *Heliyon*, vol. 10, no. 5, Mar. 2024, doi: 10.1016/j.heliyon.2024.e26845.

[9] A. El-Fergany, “Optimal allocation of multi-type distributed generators using backtracking search optimization algorithm,” *International Journal of Electrical Power and Energy Systems*, vol. 64, pp. 1197–1205, 2015, doi: 10.1016/j.ijepes.2014.09.020.

[10] E. S. Oda, A. A. Abdelsalam, M. N. Abdel-Wahab, and M. M. El-Saadawi, “Distributed generations planning using flower pollination algorithm for enhancing distribution system voltage stability,” *Ain Shams Engineering Journal*, vol. 8, no. 4, pp. 593–603, Dec. 2017, doi: 10.1016/j.asej.2015.12.001.

[11] C. H. Prasad, K. Subbaramaiah, and P. Sujatha, “Cost–benefit analysis for optimal DG placement in distribution systems by using elephant herding optimization algorithm,” *Renew Wind Water Sol*, vol. 6, no. 1, Dec. 2019, doi: 10.1186/s40807-019-0056-9.

[12] H. P. C, K. Subbaramaiah, and P. Sujatha, “Optimal DG unit placement in distribution networks by multi-objective whale optimization algorithm & its techno-economic analysis,” *Electric Power Systems Research*, vol. 214, Jan. 2023, doi: 10.1016/j.epsr.2022.108869.

[13] I. A. Mohamed and M. Kowsalya, “Optimal size and siting of multiple distributed generators in distribution system using bacterial foraging optimization,” *Swarm Evol Comput*, vol. 15, pp. 58–65, Apr. 2014, doi: 10.1016/j.swevo.2013.12.001.

[14] D. Rama Prabha and T. Jayabarathi, “Optimal placement and sizing of multiple distributed generating units in distribution networks by invasive weed optimization algorithm,” *Ain Shams Engineering Journal*, vol. 7, no. 2, pp. 683–694, Jun. 2016, doi: 10.1016/j.asej.2015.05.014.

[15] R. K. Sharma and B. K. Naick, “A Novel Artificial Rabbits Optimization Algorithm for Optimal Location and Sizing of Multiple Distributed Generation in Radial Distribution Systems,” *Arab J Sci Eng*, 2024, doi: 10.1007/s13369-023-08559-1.

[16] S. Kansal, V. Kumar, and B. Tyagi, “Hybrid approach for optimal placement of multiple DGs of multiple types in distribution networks,” *International Journal of Electrical Power and Energy Systems*, vol. 75, pp. 226–235, Feb. 2016, doi: 10.1016/j.ijepes.2015.09.002.

[17] I. Mahmoud, S. Kamel, H. Abdel-Mawgoud, L. Nasrat, and F. Jurado, “Integration of DG and Capacitor in Radial Distribution Networks Using an Efficient Hybrid Optimization Method,” *Electric Power Components and Systems*, vol. 48, no. 11, pp. 1102–1110, 2020, doi: 10.1080/15325008.2020.1831653.

[18] K. Muthukumar and S. Jayalalitha, “Optimal placement and sizing of distributed generators and shunt capacitors for power loss minimization in radial distribution networks using hybrid heuristic search optimization technique,” *International Journal of Electrical Power and Energy Systems*, vol. 78, pp. 299–319, Jun. 2016, doi: 10.1016/j.ijepes.2015.11.019.

[19] R. Bala and S. Ghosh, “Optimal position and rating of DG in distribution networks by ABC–CS from load flow solutions illustrated by fuzzy-PSO,” *Neural Comput Appl*, vol. 31, no. 2, pp. 489–507, Feb. 2019, doi: 10.1007/s00521-017-3084-7.

[20] P. Singh, N. K. Meena, S. K. Bishnoi, B. Singh, and M. Bhadu, “Hybrid Elephant Herding and Particle Swarm Optimizations for Optimal DG Integration in Distribution Networks,” *Electric Power Components and Systems*, vol. 48, no. 6–7, pp. 727–741, Aug. 2020, doi: 10.1080/15325008.2020.1797931.

[21] Z. M. Anjum, D. M. Said, M. Y. Hassan, Z. H. Leghari, and G. Sahar, “Parallel operated hybrid Arithmetic-Salp swarm optimizer for optimal allocation of multiple distributed generation units in distribution networks,” *PLoS One*, vol. 17, no. 4 April, Apr. 2022, doi: 10.1371/journal.pone.0264958.

[22] S. Sharma, S. Bhattacharjee, and A. Bhattacharya, “Quasi-Oppositional Swine Influenza Model Based Optimization with Quarantine for optimal allocation of DG in radial distribution network,” *International Journal of Electrical Power and Energy Systems*, vol. 74, pp. 348–373, Jan. 2016, doi: 10.1016/j.ijepes.2015.07.034.

[23] N. K. Meena, A. Swarnkar, N. Gupta, and K. R. Niazi, “Multi-objective Taguchi approach for optimal DG integration in distribution systems,” *IET Generation, Transmission and Distribution*, vol. 11, no. 9, pp. 2418–2428, Jun. 2017, doi: 10.1049/iet-gtd.2016.2126.

[24] S. Sultana and P. K. Roy, “Multi-objective quasi-oppositional teaching learning based optimization for optimal location of distributed generator in radial distribution systems,” *International Journal of Electrical Power and Energy Systems*, vol. 63, pp. 534–545, 2014, doi: 10.1016/j.ijepes.2014.06.031.

[25] I. A. Quadri, S. Bhowmick, and D. Joshi, “A comprehensive technique for optimal allocation of distributed energy resources in radial distribution systems,” *Appl Energy*, vol. 211, pp. 1245–1260, Feb. 2018, doi: 10.1016/j.apenergy.2017.11.108.

[26] I. A. Quadri, S. Bhowmick, and D. Joshi, “A hybrid teaching–learning-based optimization technique for optimal DG sizing and placement in radial distribution systems,” *Soft comput*, vol. 23, no. 20, pp. 9899–9917, Oct. 2019, doi: 10.1007/s00500-018-3544-8.

[27] A. Parizad and K. Hatziadoniu, “Security/stability-based Pareto optimal solution for distribution networks planning implementing NSGAII/FDMT,” *Energy*, vol. 192, Feb. 2020, doi: 10.1016/j.energy.2019.116644.

[28] A. Selim, S. Kamel, and F. Jurado, “Efficient optimization technique for multiple DG allocation in distribution networks,” *Applied Soft Computing Journal*, vol. 86, Jan. 2020, doi: 10.1016/j.asoc.2019.105938.

[29] T. H. B. Huy, D. N. Vo, K. H. Truong, and T. Van Tran, “Optimal Distributed Generation Placement in Radial Distribution Networks Using Enhanced Search Group Algorithm,” *IEEE Access*, vol. 11, pp. 103288–103305, 2023, doi: 10.1109/ACCESS.2023.3316725.

[30] A. Selim, M. H. Hassan, S. Kamel, and A. G. Hussien, “Allocation of distributed generator in power networks through an enhanced jellyfish search algorithm,” *Energy Reports*, vol. 10, pp. 4761–4780, Nov. 2023, doi: 10.1016/j.egyr.2023.11.032.

[31] M. A. Elseify, F. A. Hashim, A. G. Hussien, and S. Kamel, “Single and multi-objectives based on an improved golden jackal optimization algorithm for simultaneous integration of multiple capacitors and multi-type DGs in distribution systems,” *Appl Energy*, vol. 353, Jan. 2024, doi: 10.1016/j.apenergy.2023.122054.

[32] D. Tian, X. Zhao, and Z. Shi, “Chaotic particle swarm optimization with sigmoid-based acceleration coefficients for numerical function optimization,” *Swarm Evol Comput*, vol. 51, Dec. 2019, doi: 10.1016/j.swevo.2019.100573.

[33] A. Noori, Y. Zhang, N. Nouri, and M. Hajivand, “Hybrid allocation of capacitor and distributed static compensator in radial distribution networks using multi-objective improved golden ratio optimization based on fuzzy decision making,” *IEEE Access*, vol. 8, pp. 162180–162195, 2020, doi: 10.1109/ACCESS.2020.2993693.

[34] M. Chakravorty and D. Das, “Voltage stability analysis of radial distribution networks.” [Online]. Available: www.elsevier.com/locate/ijepes

[35] A. Ratnaweera, S. K. Halgamuge, and H. C. Watson, “Self-organizing hierarchical particle swarm optimizer with time-varying acceleration coefficients,” *IEEE Transactions on Evolutionary Computation*, vol. 8, no. 3, pp. 240–255, Jun. 2004, doi: 10.1109/TEVC.2004.826071.

[36] R. A. Lone, S. Javed Iqbal, and A. S. Anees, “Optimal location and sizing of distributed generation for distribution systems: An improved analytical technique,” *Int J Green Energy*, 2023, doi: 10.1080/15435075.2023.2207638.

[37] A. Bayat and A. Bagheri, “Optimal active and reactive power allocation in distribution networks using a novel heuristic approach,” *Appl Energy*, vol. 233–234, pp. 71–85, Jan. 2019, doi: 10.1016/j.apenergy.2018.10.030.